

ADVERSARIAL EXAMPLES IN THE PHYSICAL WORLD

Alexey Kurakin
Google Brain
kurakin@google.com

Ian J. Goodfellow
OpenAI
ian@openai.com

Samy Bengio
Google Brain
bengio@google.com

ABSTRACT

Most existing machine learning classifiers are highly vulnerable to adversarial examples. An adversarial example is a sample of input data which has been modified very slightly in a way that is intended to cause a machine learning classifier to misclassify it. In many cases, these modifications can be so subtle that a human observer does not even notice the modification at all, yet the classifier still makes a mistake. Adversarial examples pose security concerns because they could be used to perform an attack on machine learning systems, even if the adversary has no access to the underlying model. Up to now, all previous work have assumed a threat model in which the adversary can feed data directly into the machine learning classifier. This is not always the case for systems operating in the physical world, for example those which are using signals from cameras and other sensors as an input. This paper shows that even in such physical world scenarios, machine learning systems are vulnerable to adversarial examples. We demonstrate this by feeding adversarial images obtained from cell-phone camera to an ImageNet Inception classifier and measuring the classification accuracy of the system. We find that a large fraction of adversarial examples are classified incorrectly even when perceived through the camera.

1 INTRODUCTION

Recent advances in machine learning and deep neural networks enabled researchers to solve multiple important practical problems like image, video, text classification and others (Krizhevsky et al., 2012; Hinton et al., 2012; Bahdanau et al., 2015).

However, machine learning models are often vulnerable to adversarial manipulation of their input intended to cause incorrect classification (Dalvi et al., 2004). In particular, neural networks and many other categories of machine learning models are highly vulnerable to attacks based on small modifications of the input to the model at test time (Biggio et al., 2013; Szegedy et al., 2014; Goodfellow et al., 2014; Papernot et al., 2016b).

The problem can be summarized as follows. Let's say there is a machine learning system M and input sample C which we call a clean example. Let's assume that sample C is correctly classified by the machine learning system, i.e. $M(C) = y_{true}$. It's possible to construct an adversarial example A which is perceptually indistinguishable from C but is classified incorrectly, i.e. $M(A) \neq y_{true}$. These adversarial examples are misclassified far more often than examples that have been perturbed by noise, even if the magnitude of the noise is much larger than the magnitude of the adversarial perturbation (Szegedy et al., 2014).

Adversarial examples pose potential security threats for practical machine learning applications. In particular, Szegedy et al. (2014) showed that an adversarial example that was designed to be misclassified by a model M_1 is often also misclassified by a model M_2 . This adversarial example transferability property means that it is possible to generate adversarial examples and perform a misclassification attack on a machine learning system without access to the underlying model. Papernot et al. (2016a) and Papernot et al. (2016b) demonstrated such attacks in realistic scenarios.

However all prior work on adversarial examples for neural networks made use of a threat model in which the attacker can supply input directly to the machine learning model. Thus adversarial attacks rely on fine-grained modifications of input data.

Such a threat model can describe some scenarios in which attacks can take place entirely within a computer, such as evading spam filters or malware detectors (Biggio et al., 2013; Nelson et al.). However, many practical machine learning systems operate in the physical world. Possible examples include but are not limited to: robots perceiving world through cameras and other sensors, video surveillance systems, and mobile applications for image or sound classification. In such scenarios the adversary cannot rely on the ability of fine-grained per-pixel modifications of the input data. The following question thus arises: is it still possible to craft adversarial examples and perform adversarial attacks on machine learning systems which are operating in the physical world and perceiving data through various sensors, rather than digital representation?

Some prior work has addressed the problem of physical attacks against machine learning systems, but not in the context of fooling neural networks by making very small perturbations of the input. For example, Carlini et al. (2016) demonstrate an attack that can create audio inputs that mobile phones recognize as containing intelligible voice commands, but that humans hear as an unintelligible voice. Face recognition systems based on photos are vulnerable to replay attacks, in which a previously captured image of an authorized user’s face is presented to the camera instead of an actual face (Smith et al., 2015). Adversarial examples could in principle be applied in either of these physical domains. An adversarial example for the voice command domain would consist of a recording that seems to be innocuous to a human observer (such as a song) but contains voice commands recognized by a machine learning algorithm. An adversarial example for the face recognition domain might consist of very subtle markings applied to a person’s face, so that a human observer would recognize their identity correctly, but a machine learning system would recognize them as being a different person.

In this paper we explore the possibility of creating adversarial examples in the physical world for image classification tasks. For this purpose we conducted an experiment with a pre-trained ImageNet Inception classifier (Szegedy et al., 2015). We generated adversarial examples for this model, then we fed these examples to the classifier through a cell-phone camera and measured the classification accuracy. This scenario is a simple physical world system which perceives data through a camera and then runs image classification. We found that a large fraction of adversarial examples generated for the original model remain misclassified even when perceived through a camera.¹

Surprisingly, our attack methodology required no modification to account for the presence of the camera—the simplest possible attack of using adversarial examples crafted for the Inception model resulted in adversarial examples that successfully transferred to the union of the camera and Inception. Our results thus provide a lower bound on the attack success rate that could be achieved with more specialized attacks that explicitly model the camera while crafting the adversarial example.

One limitation of our results is that we have assumed a threat model under which the attacker has full knowledge of the model architecture and parameter values. This is primarily so that we can use a single Inception v3 model in all experiments, without having to devise and train a different high-performing model. The adversarial example transfer property implies that our results are likely to extend trivially to the scenario where the attacker does not have access to the model description (Szegedy et al., 2014; Goodfellow et al., 2014; Papernot et al., 2016b).

¹ Dileep George noticed that another kind of adversarially constructed input, designed to have no true class yet be categorized as belonging to a specific class, fooled convolutional networks when photographed, in a less systematic experiments. As of August 19, 2016 it was mentioned in Figure 6 at <http://www.evolvingai.org/fooling>

To better understand how the non-trivial image transformations caused by the camera affect adversarial example transferability, we conducted a series of additional experiments where we studied how adversarial examples transfer across several specific kinds of synthetic image transformations.

The rest of the paper is structured as follows: In Section 2, we review different methods which we used to generate adversarial examples. This is followed in Section 3 by details about our “physical world” experimental set-up and results. Finally, Section 4 describes our experiments with various artificial image transformations (like changing brightness, contrast, etc...) and how they affect adversarial examples.

2 METHODS GENERATING ADVERSARIAL IMAGES

This section describes different methods to generate adversarial examples which we have used in the experiments. It is important to note that none of the described methods guarantees that generated image will be misclassified. Nevertheless we call all of the generated images “adversarial images”.

In the remaining of the paper we use the following notation:

- \mathbf{X} - an image, which is typically 3-D tensor (width \times height \times depth). In this paper, we assume that the values of the pixels are integer numbers in the range $[0, 255]$.
- y_{true} - true class for the image \mathbf{X} .
- $J(\mathbf{X}, y)$ - cross-entropy cost function of the neural network, given image \mathbf{X} and class y . We intentionally omit network weights (and other parameters) θ in the cost function because we assume they are fixed (to the value resulting from training the machine learning model) in the context of the paper. For neural networks with a softmax output layer, the cross-entropy cost function applied to integer class labels equals the negative log-probability of the true class given the image: $J(\mathbf{X}, y) = -\log p(y|\mathbf{X})$, this relationship will be used below.
- $Clip_{X,\epsilon}\{\mathbf{X}'\}$ - function which performs per-pixel clipping of the image \mathbf{X}' , so the result will be in L_∞ ϵ -neighbourhood of the source image \mathbf{X} . The exact clipping equation is as follows:

$$Clip_{X,\epsilon}\{\mathbf{X}'\}(x, y, z) = \min\left\{255, \mathbf{X}(x, y, z) + \epsilon, \max\{0, \mathbf{X}(x, y, z) - \epsilon, \mathbf{X}'(x, y, z)\}\right\}$$

where $\mathbf{X}(x, y, z)$ is the value of channel z of the image \mathbf{X} at coordinates (x, y) .

2.1 FAST METHOD

One of the simplest methods to generate adversarial images, described in (Goodfellow et al., 2014), is motivated by linearizing the cost function and solving for the perturbation that maximizes the cost subject to an L_∞ constraint. This may be accomplished in closed form, for the cost of one call to back-propagation:

$$\mathbf{X}^{adv} = \mathbf{X} + \epsilon \text{sign}(\nabla_{\mathbf{X}} J(\mathbf{X}, y_{true}))$$

where ϵ is a hyper-parameter to be chosen.

In this paper we refer to this method as “fast” because it does not require an iterative procedure to compute adversarial examples, and thus is much faster than other considered methods.

2.2 BASIC ITERATIVE METHOD

We introduce a straightforward way to extend the “fast” method—we apply it multiple times with small step size, and clip pixel values of intermediate results after each step to ensure that they are in an ϵ -neighbourhood of the original image:

$$\mathbf{X}_0^{adv} = \mathbf{X}, \quad \mathbf{X}_{N+1}^{adv} = Clip_{X,\epsilon}\left\{\mathbf{X}_N^{adv} + \alpha \text{sign}(\nabla_{\mathbf{X}} J(\mathbf{X}_N^{adv}, y_{true}))\right\}$$

In our experiments we used $\alpha = 1$, i.e. we changed the value of each pixel only by 1 on each step. We selected the number of iterations to be $\min(\epsilon + 4, 1.25\epsilon)$. This amount of iterations was chosen

heuristically; it is sufficient for the adversarial example to reach the edge of the ϵ max-norm ball but restricted enough to keep the computational cost of experiments manageable.

Below we refer to this method as “basic iterative” method.

2.3 ITERATIVE LEAST-LIKELY CLASS METHOD

Both methods we have described so far simply try to increase the cost of the correct class, without specifying which of the incorrect classes the model should select. Such methods are sufficient for application to datasets such as MNIST and CIFAR-10, where the number of classes is small and all classes are highly distinct from each other. On ImageNet, with a much larger number of classes and the varying degrees of significance in the difference between classes, these methods can result in uninteresting misclassifications, such as mistaking one breed of sled dog for another breed of sled dog. In order to create more interesting mistakes, we introduce the *iterative least-likely class method*. This iterative method tries to make an adversarial image which will be classified as a specific desired target class. For desired class we chose the least-likely class according to the prediction of the trained network on image \mathbf{X} :

$$y_{LL} = \arg \min_y \{p(y|\mathbf{X})\}.$$

For a well-trained classifier, the least-likely class is usually highly dissimilar from the true class, so this attack method results in more interesting mistakes, such as mistaking a dog for an airplane.

To make an adversarial image which is classified as y_{LL} we maximize $\log p(y_{LL}|\mathbf{X})$ by making iterative steps in the direction of $\text{sign}\{\nabla_X \log p(y_{LL}|\mathbf{X})\}$. This last expression equals $\text{sign}\{-\nabla_X J(\mathbf{X}, y_{LL})\}$ for neural networks with cross-entropy loss. Thus we have the following procedure:

$$\mathbf{X}_0^{adv} = \mathbf{X}, \quad \mathbf{X}_{N+1}^{adv} = \text{Clip}_{X,\epsilon} \{ \mathbf{X}_N^{adv} - \alpha \text{sign}(\nabla_X J(\mathbf{X}_N^{adv}, y_{LL})) \}$$

For this iterative procedure we used the same α and same number of iterations as for the basic iterative method.

Below we refer to this method as the “least likely class” method or shortly “l.l. class”.

2.4 COMPARISON OF METHODS OF GENERATING ADVERSARIAL EXAMPLES

As mentioned above, it is not guaranteed that an adversarial image will actually be misclassified—sometimes the attacker wins, and sometimes the machine learning model wins. We did an experimental comparison of adversarial methods to understand the actual classification accuracy on the generated images as well as the types of perturbations exploited by each of the methods.

The experiments were performed on all 50,000 validation samples from the ImageNet dataset (Russakovsky et al., 2014) using a pre-trained Inception v3 classifier (Szegedy et al., 2015). For each validation image, we generated adversarial examples using different methods and different values of ϵ . For each pair of method and ϵ , we computed the classification accuracy on all 50,000 images. Also, we computed the accuracy on all clean images, which we used as a baseline.

Examples of generated adversarial images are provided in Figures 1 and 2. Top-1 and top-5 classification accuracy on clean and adversarial images are summarized in Figure 3.

As shown in Figure 3, the fast method decreases top-1 accuracy by a factor of two and top-5 accuracy by about 40% even with the smallest values of ϵ . As we increase ϵ , accuracy on adversarial images generated by the fast method stays on approximately the same level until $\epsilon = 32$ and then slowly decreases to almost 0 as ϵ grows to 128. This could be explained by the fact that the fast method adds ϵ -scaled noise to each image, thus higher values of ϵ essentially destroys the content of the image and makes it unrecognisable even by humans, see Figure 1.

Iterative methods exploit much finer perturbations which do not destroy the image even with higher ϵ , see Figure 2.

The basic iterative method is able to produce better adversarial images when $\epsilon < 48$, however as we increase ϵ it is unable to improve.

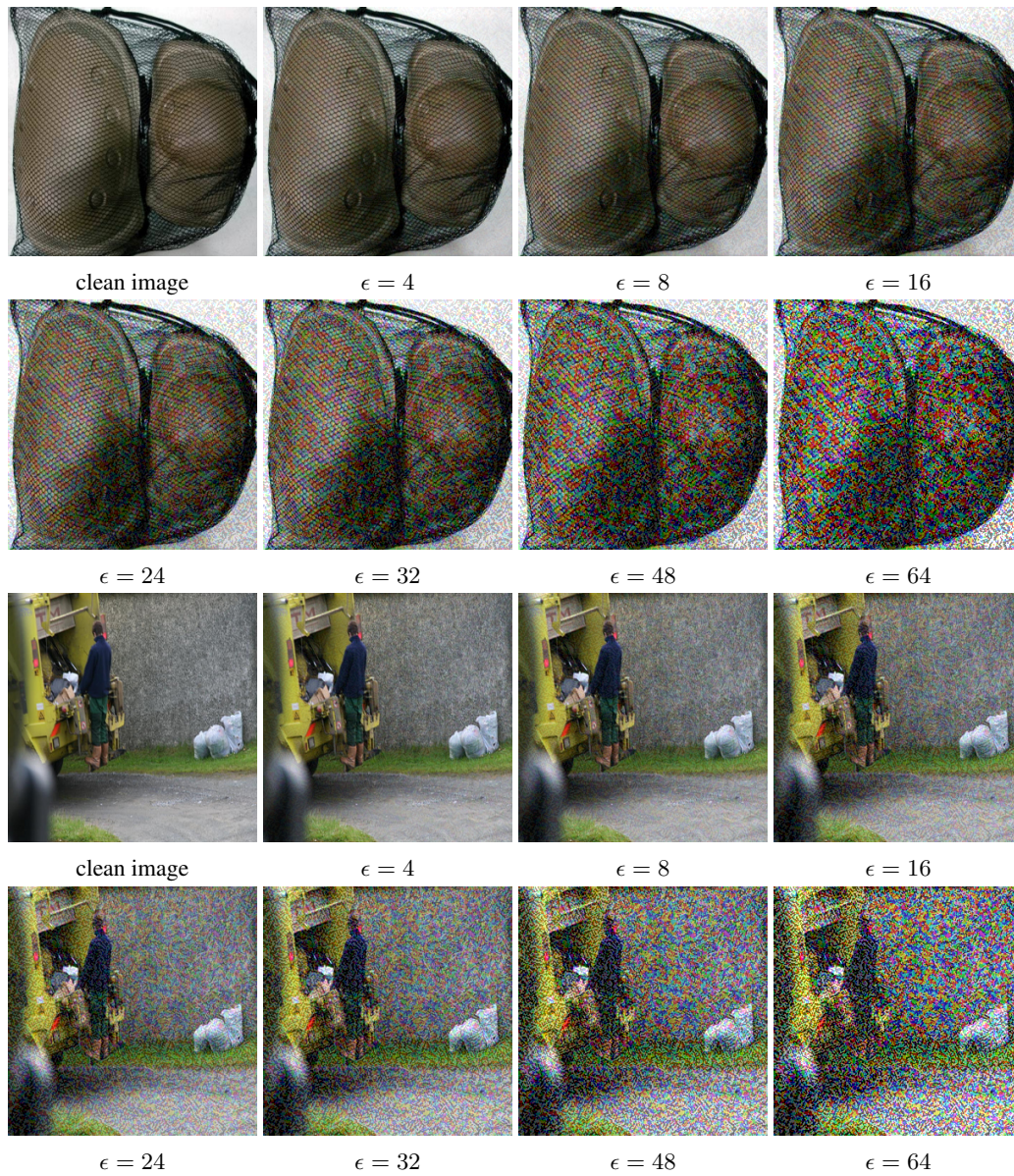


Figure 1: Comparison of images resulting from an adversarial perturbation using the “fast” method. The top image is a “knee pad” while the bottom one is a “garbage truck”. In both cases clean images are classified correctly and adversarial images are misclassified for all considered ϵ .



Figure 2: Comparison of different adversarial methods with $\epsilon = 32$. Perturbations generated by iterative methods are finer compared to the fast method. Also iterative methods do not always select a point on the border of ϵ -neighbourhood as an adversarial image.

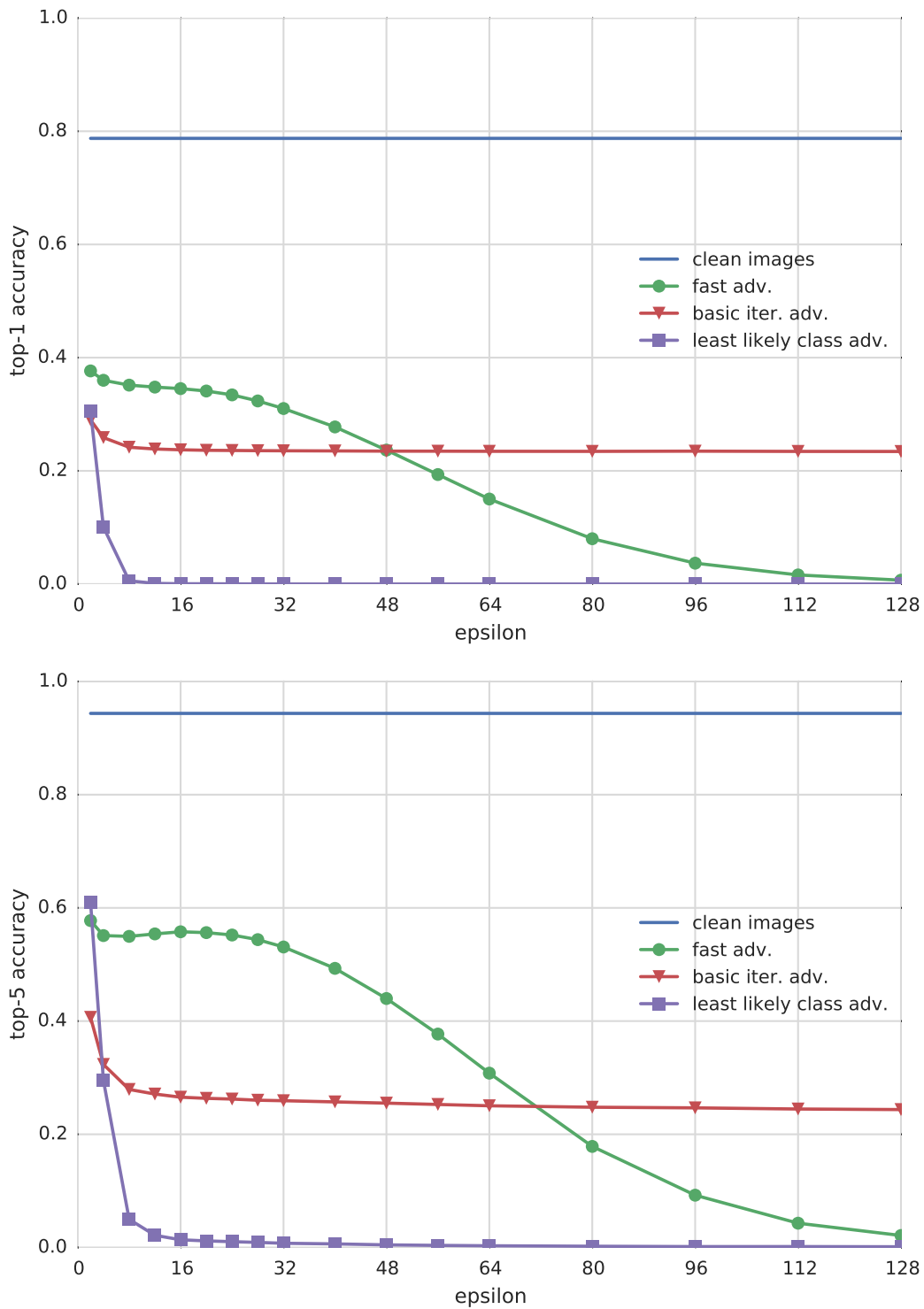


Figure 3: Top-1 and top-5 accuracy of Inception v3 under attack by different adversarial methods and different ϵ compared to “clean images” — unmodified images from the dataset. The Accuracy was computed on all 50,000 validation images from the ImageNet dataset. In these experiments ϵ varies from 2 to 128.



Figure 4: Experimental setup: (a) generated printout which contains pairs of clean and adversarial images, as well as QR codes to help automatic cropping; (b) photo of the printout made by a cellphone camera; (c) automatically cropped image from the photo.

The “least likely class” method destroys the correct classification of most images even when ϵ is relatively small.

We limit all further experiments to $\epsilon \leq 16$ because such perturbations are only perceived as a small noise (if perceived at all), and adversarial methods are able to produce a significant number of misclassified examples in this ϵ -neighbourhood of clean images.

3 PHOTOS OF ADVERSARIAL EXAMPLES

3.1 DESTRUCTION RATE OF ADVERSARIAL IMAGES

To study the influence of arbitrary transformations on adversarial images we introduce the notion of destruction rate. It can be described as the fraction of adversarial images which are no longer misclassified after the transformations. The formal definition is the following:

$$d = \frac{\sum_{k=1}^n C(\mathbf{X}^k, y_{true}^k) \overline{C(\mathbf{X}_{adv}^k, y_{true}^k)} C(T(\mathbf{X}_{adv}^k), y_{true}^k)}{\sum_{k=1}^n C(\mathbf{X}^k, y_{true}^k) \overline{C(\mathbf{X}_{adv}^k, y_{true}^k)}} \quad (1)$$

where n is the number of images used to compute the destruction rate, \mathbf{X}^k is an image from the dataset, y_{true}^k is the true class of this image, and \mathbf{X}_{adv}^k is the corresponding adversarial image. The function $T(\bullet)$ is an arbitrary image transformation—in this article, we study a variety of transformations, including printing the image and taking a photo of the result. The function $C(\mathbf{X}, y)$ is an indicator function which returns whether the image was classified correctly:

$$C(\mathbf{X}, y) = \begin{cases} 1, & \text{if image } \mathbf{X} \text{ is classified as } y; \\ 0, & \text{otherwise.} \end{cases}$$

We denote the binary negation of this indicator value as $\overline{C(\mathbf{X}, y)}$, which is computed as $\overline{C(\mathbf{X}, y)} = 1 - C(\mathbf{X}, y)$.

3.2 EXPERIMENTAL SETUP

To explore the possibility of physical adversarial examples we ran a series of experiments with photos of adversarial examples. We printed clean and adversarial images, took photos of the printed

pages, and cropped the printed images from the photos of the full page. We can think of this as a black box transformation that we refer to as “photo transformation”.

We computed the accuracy on clean and adversarial images before and after the photo transformation as well as the destruction rate of adversarial images subjected to photo transformation.

The experimental procedure was as follows:

1. Print the image, see Figure 4a. In order to reduce the amount of manual work, we printed multiple pairs of clean and adversarial examples on each sheet of paper. Also, QR codes were put into corners of the printout to facilitate automatic cropping.
 - (a) All generated pictures of printouts (Figure 4a) were saved in lossless PNG format.
 - (b) Batches of PNG printouts were converted to multi-page PDF file using the convert tool from the ImageMagick suite with the default settings: `convert *.png output.pdf`
 - (c) Generated PDF files were printed using a *Ricoh MP C5503* office printer. Each page of PDF file was automatically scaled to fit the entire sheet of paper using the default printer scaling. The printer resolution was set to 600dpi.
2. Take a photo of the printed image using a cell phone camera (Nexus 5x), see Figure 4b.
3. Automatically crop and warp validation examples from the photo, so they would become squares of the same size as source images, see Figure 4c:
 - (a) Detect values and locations of four QR codes in the corners of the photo. The QR codes encode which batch of validation examples is shown on the photo. If detection of any of the corners failed, the entire photo was discarded and images from the photo were not used to calculate accuracy. We observed that no more than 10% of all images were discarded in any experiment and typically the number of discarded images was about 3% to 6%.
 - (b) Warp photo using perspective transform to move location of QR codes into pre-defined coordinates.
 - (c) After the image was warped, each example has known coordinates and can easily be cropped from the image.
4. Run classification on transformed and source images. Compute accuracy and destruction rate of adversarial images.

This procedure involves manually taking photos of the printed pages, without careful control of lighting, camera angle, distance to the page, etc. This is intentional; it introduces nuisance variability that has the potential to destroy adversarial perturbations that depend on subtle, fine co-adaptation of exact pixel values. That being said, we did not intentionally seek out extreme camera angles or lighting conditions. All photos were taken in normal indoor lighting with the camera pointed approximately straight at the page.

For each combination of adversarial example generation method and ϵ we conducted two sets of experiments:

- **Average case.** To measure the average case performance, we randomly selected 102 images to use in one experiment with a given ϵ and adversarial method. This experiment estimates how often an adversary would succeed on randomly chosen photos—the world chooses an image randomly, and the adversary attempts to cause it to be misclassified.
- **Prefiltered case.** To study a more aggressive attack, we performed experiments in which the images are prefiltered. Specifically, we selected 102 images such that all clean images are classified correctly, and all adversarial images (before photo transformation) are classified incorrectly (both top-1 and top-5 classification). In addition we used a confidence threshold for the top prediction: $p(y_{predicted}|\mathbf{X}) \geq 0.8$, where $y_{predicted}$ is the class predicted by the network for image \mathbf{X} . This experiment measures how often an adversary would succeed when the adversary can choose the original image to attack. Under our threat model, the adversary has access to the model parameters and architecture, so the attacker can always run inference to determine whether an attack will succeed in the absence of photo transformation. The attacker might expect to do the best by choosing to

make attacks that succeed in this initial condition. The victim then takes a new photo of the physical object that the attacker chooses to display, and the photo transformation can either preserve the attack or destroy it.

3.3 EXPERIMENTAL RESULTS ON PHOTOS OF ADVERSARIAL IMAGES

Table 1: Accuracy on photos of adversarial images in the average case (randomly chosen images).

Adversarial method	Photos				Source images			
	Clean images		Adv. images		Clean images		Adv. images	
	top-1	top-5	top-1	top-5	top-1	top-5	top-1	top-5
fast $\epsilon = 16$	79.8%	91.9%	36.4%	67.7%	85.3%	94.1%	36.3%	58.8%
fast $\epsilon = 8$	70.6%	93.1%	49.0%	73.5%	77.5%	97.1%	30.4%	57.8%
iter. basic $\epsilon = 16$	72.9%	89.6%	49.0%	75.0%	81.4%	95.1%	28.4%	31.4%
iter. basic $\epsilon = 8$	72.5%	93.1%	51.0%	87.3%	73.5%	93.1%	26.5%	31.4%
l.l. class $\epsilon = 16$	71.1%	90.0%	60.0%	83.3%	79.4%	96.1%	1.0%	1.0%
l.l. class $\epsilon = 8$	76.5%	94.1%	69.6%	92.2%	78.4%	98.0%	0.0%	6.9%

Table 2: Accuracy on photos of adversarial images in the prefiltered case (clean image correctly classified, adversarial image confidently incorrectly classified).

Adversarial method	Photos				Source images			
	Clean images		Adv. images		Clean images		Adv. images	
	top-1	top-5	top-1	top-5	top-1	top-5	top-1	top-5
fast $\epsilon = 16$	81.8%	97.0%	5.1%	39.4%	100.0%	100.0%	0.0%	0.0%
fast $\epsilon = 8$	77.1%	95.8%	14.6%	70.8%	100.0%	100.0%	0.0%	0.0%
iter. basic $\epsilon = 16$	93.3%	97.8%	60.0%	87.8%	100.0%	100.0%	0.0%	0.0%
iter. basic $\epsilon = 8$	89.2%	98.0%	64.7%	91.2%	100.0%	100.0%	0.0%	0.0%
l.l. class $\epsilon = 16$	95.8%	100.0%	87.5%	97.9%	100.0%	100.0%	0.0%	0.0%
l.l. class $\epsilon = 8$	96.0%	100.0%	88.9%	97.0%	100.0%	100.0%	0.0%	0.0%

Table 3: Adversarial image destruction rate with photos.

Adversarial method	Average case		Prefiltered case	
	top-1	top-5	top-1	top-5
fast $\epsilon = 16$	12.5%	40.0%	5.1%	39.4%
fast $\epsilon = 8$	33.3%	40.0%	14.6%	70.8%
iter. basic $\epsilon = 16$	40.4%	69.4%	60.0%	87.8%
iter. basic $\epsilon = 8$	52.1%	90.5%	64.7%	91.2%
l.l. class $\epsilon = 16$	72.2%	85.1%	87.5%	97.9%
l.l. class $\epsilon = 8$	86.3%	94.6%	88.9%	97.0%

Results of the photo transformation experiment are summarized in Tables 1, 2 and 3.

We found that “fast” adversarial images are more robust to photo transformation compared to iterative methods. This could be explained by the fact that iterative methods exploit more subtle kind of perturbations, and these subtle perturbations are more likely to be destroyed by photo transformation.

One unexpected result is that in some cases the adversarial destruction rate in the “prefiltered case” was higher compared to the “average case”. In the case of the iterative methods, even the total success rate was lower for prefiltered images rather than randomly selected images. This suggests that, to obtain very high confidence, iterative methods often make subtle co-adaptations that are not able to survive photo transformation.

Overall, the results show that some fraction of adversarial examples stays misclassified even after a non-trivial transformation: the photo transformation. This demonstrates the possibility of physical adversarial examples. For example, an adversary using the fast method with $\epsilon = 16$ could expect that about 2/3 of the images would be top-1 misclassified and about 1/3 of the images would be top-5 misclassified. Thus by generating enough adversarial images, the adversary could expect to cause far more misclassification than would occur on natural inputs.

4 ARTIFICIAL IMAGE TRANSFORMATIONS

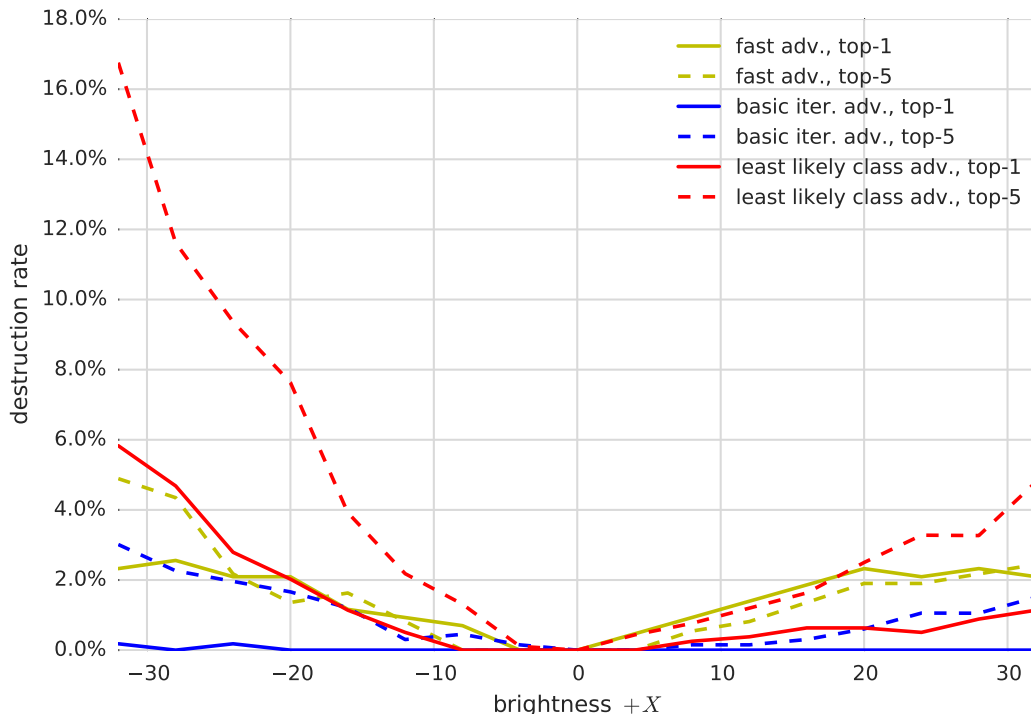


Figure 5: Comparison of adversarial destruction rates for various adversarial methods for transformation which changes brightness. All experiments were done with $\epsilon = 16$.

Photo transformations described in the previous section could be considered as some combination of much simpler image transformations. Thus to better understand what is going on we conducted a series of experiments to measure the adversarial destruction rate on artificial image transformations. We explored the following set of transformations: change of contrast and brightness, Gaussian blur, Gaussian noise, and JPEG encoding.

For this set of experiments we used a subset of 1,000 images randomly selected from the validation set. This subset of 1,000 was selected once, thus all experiments from this section used the same subset of images. We performed experiments for multiple pairs of adversarial method and transformation. For each given pair of transformation and adversarial method we computed adversarial examples, applied the transformation to the adversarial examples, and then computed the destruction rate according to Equation (1).

The results² for various transformations and adversarial methods with $\epsilon = 16$ are summarized in Figures 5, 6, 7, 8 and 9. The following general observations can be drawn:

²To save space, we omit several experiments we performed that did not have unique and interesting results. For example, the composition of several JPEG transforms was similar to a single JPEG transform, median blur was similar to Gaussian blur, etc.

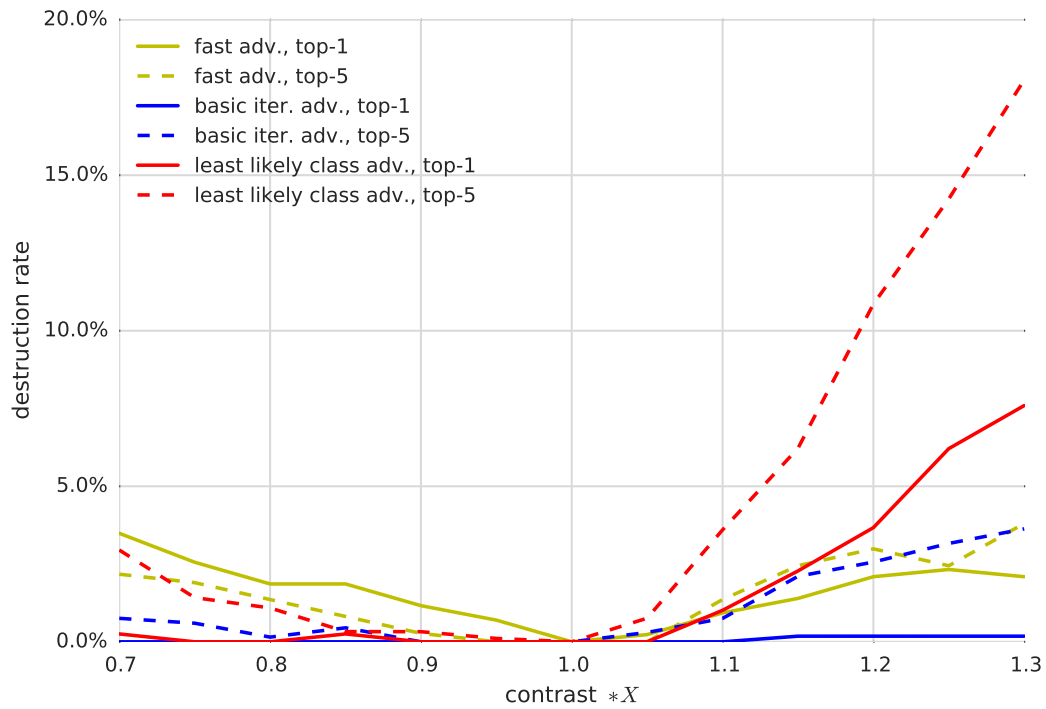


Figure 6: Comparison of adversarial destruction rates for various adversarial methods for transformation which changes contrast. All experiments were done with $\epsilon = 16$.

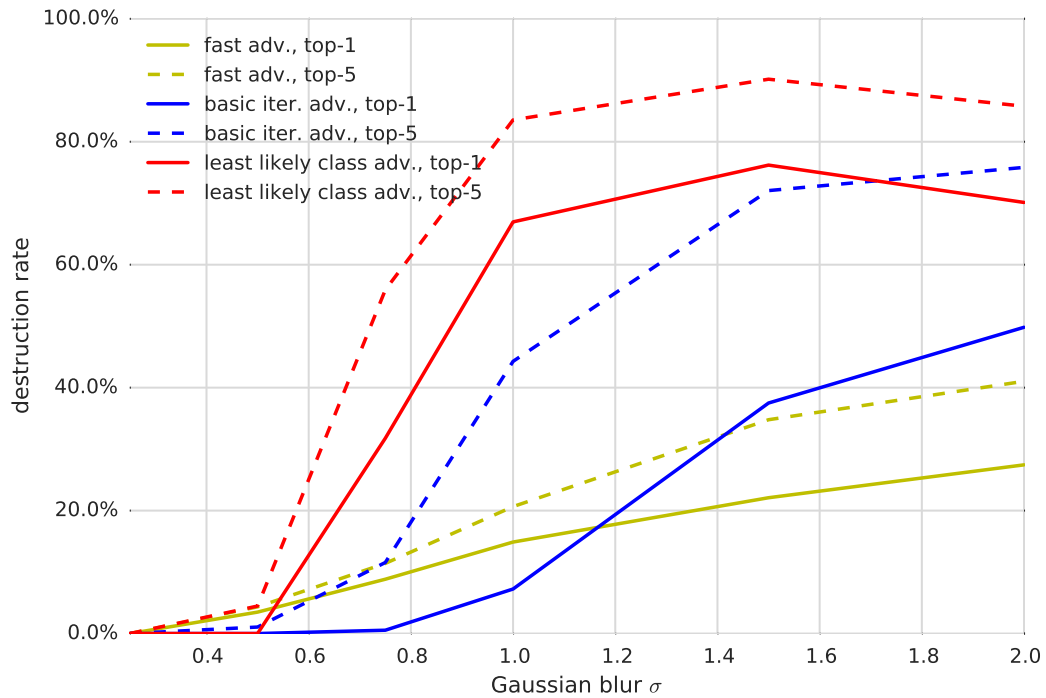


Figure 7: Comparison of adversarial destruction rates for various adversarial methods for Gaussian blur transformation. All experiments were done with $\epsilon = 16$.

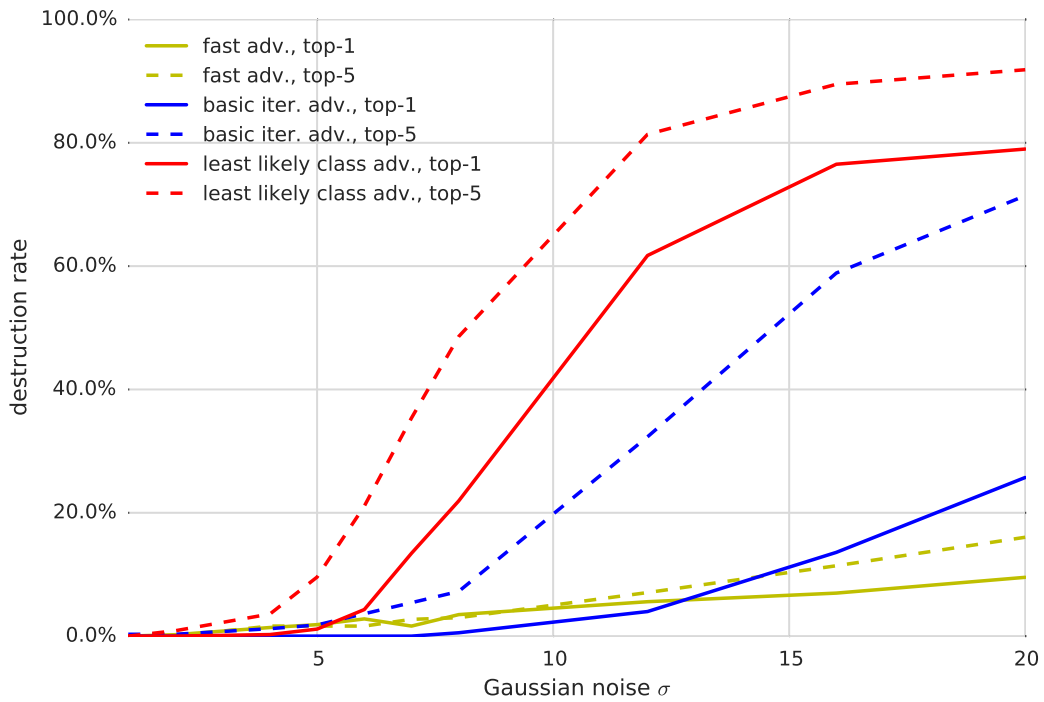


Figure 8: Comparison of adversarial destruction rates for various adversarial methods for Gaussian noise transformation. All experiments were done with $\epsilon = 16$.

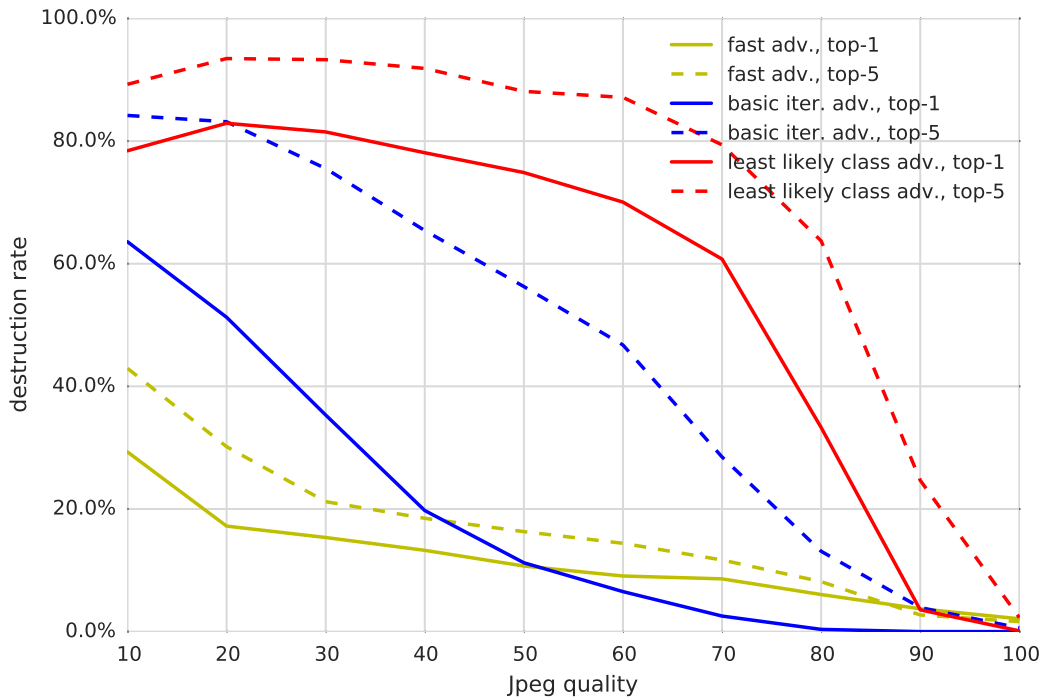


Figure 9: Comparison of adversarial destruction rates for various adversarial methods for JPEG encoding transformation. All experiments were done with $\epsilon = 16$.

- Adversarial examples generated by the fast method are the most robust to transformations, and adversarial examples generated by the iterative least-likely class method are the least robust. This coincides with our results on photo transformation.
- The top-5 destruction rate is typically higher than top-1 destruction rate. This can be explained by the fact that in order to “destroy” top-5 adversarial examples, a transformation has to push the correct class labels into one of the top-5 predictions. However in order to destroy top-1 adversarial examples we have to push the correct label to be top-1 prediction, which is a strictly stronger requirement.
- Changing brightness and contrast does not affect adversarial examples much. The destruction rate on fast and basic iterative adversarial examples is less than 5%, and for the iterative least-likely class method it is less than 20%.
- Blur, noise and JPEG encoding have a higher destruction rate than changes of brightness and contrast. In particular, the destruction rate for iterative methods could reach 80% – 90%. However none of these transformations destroy 100% of adversarial examples, which coincides with the “photo transformation” experiment.

5 CONCLUSION

In this paper we explored the possibility of creating adversarial examples for machine learning systems which operate in the physical world. We used images taken from a cell-phone camera as an input to an Inception v3 image classification neural network. We showed that in such a set-up, a significant fraction of adversarial images crafted using the original network are misclassified even when fed to the classifier through the camera. This finding demonstrates the possibility of adversarial examples for machine learning systems in the physical world. In future work, we expect that it will be possible to demonstrate attacks using other kinds of physical objects besides images printed on paper, attacks against different kinds of machine learning systems, such as sophisticated reinforcement learning agents, attacks performed without access to the model’s parameters and architecture (presumably using the transfer property), and physical attacks that achieve a higher success rate by explicitly modeling the physical transformation during the adversarial example construction process. We also hope that future work will develop effective methods for defending against such attacks.

REFERENCES

- Bahdanau, Dzmitry, Cho, Kyunghyun, and Bengio, Yoshua. Neural machine translation by jointly learning to align and translate. In *ICLR’2015*, *arXiv:1409.0473*, 2015.
- Biggio, Battista, Corona, Igino, Maiorca, Davide, Nelson, Blaine, Šrndić, Nedim, Laskov, Pavel, Giacinto, Giorgio, and Roli, Fabio. Evasion attacks against machine learning at test time. In *Joint European Conference on Machine Learning and Knowledge Discovery in Databases*, pp. 387–402. Springer, 2013.
- Carlini, Nicholas, Mishra, Pratyush, Vaidya, Tavish, Zhang, Yuankai, Sherr, Micah, Shields, Clay, Wagner, David, and Zhou, Wenchao. Hidden voice commands. In *25th USENIX Security Symposium (USENIX Security 16)*, Austin, TX, August 2016. USENIX Association. URL <https://www.usenix.org/conference/usenixsecurity16/technical-sessions/presentation/carlini>.
- Dalvi, Nilesh, Domingos, Pedro, Sanghai, Sumit, Verma, Deepak, et al. Adversarial classification. In *Proceedings of the tenth ACM SIGKDD international conference on Knowledge discovery and data mining*, pp. 99–108. ACM, 2004.
- Goodfellow, Ian J., Shlens, Jonathon, and Szegedy, Christian. Explaining and harnessing adversarial examples. *CoRR*, abs/1412.6572, 2014. URL <http://arxiv.org/abs/1412.6572>.
- Hinton, Geoffrey, Deng, Li, Yu, Dong, Dahl, George, rahman Mohamed, Abdel, Jaitly, Navdeep, Senior, Andrew, Vanhoucke, Vincent, Nguyen, Patrick, Sainath, Tara, and Kingsbury, Brian. Deep neural networks for acoustic modeling in speech recognition. *Signal Processing Magazine*, 2012.

- Krizhevsky, Alex, Sutskever, Ilya, and Hinton, Geoffrey. ImageNet classification with deep convolutional neural networks. In *Advances in Neural Information Processing Systems 25 (NIPS'2012)*. 2012.
- Nelson, Blaine, Barreno, Marco, Chi, Fuching Jack, Joseph, Anthony D, Rubinstein, Benjamin IP, Saini, Udam, Sutton, Charles A, Tygar, J Doug, and Xia, Kai. Exploiting machine learning to subvert your spam filter.
- Papernot, N., McDaniel, P., and Goodfellow, I. Transferability in Machine Learning: from Phenomena to Black-Box Attacks using Adversarial Samples. *ArXiv e-prints*, May 2016b. URL <http://arxiv.org/abs/1605.07277>.
- Papernot, Nicolas, McDaniel, Patrick Drew, Goodfellow, Ian J., Jha, Somesh, Celik, Z. Berkay, and Swami, Ananthram. Practical black-box attacks against deep learning systems using adversarial examples. *CoRR*, abs/1602.02697, 2016a. URL <http://arxiv.org/abs/1602.02697>.
- Russakovsky, Olga, Deng, Jia, Su, Hao, Krause, Jonathan, Satheesh, Sanjeev, Ma, Sean, Huang, Zhiheng, Karpathy, Andrej, Khosla, Aditya, Bernstein, Michael, et al. Imagenet large scale visual recognition challenge. *arXiv preprint arXiv:1409.0575*, 2014.
- Smith, Daniel F, Wiliem, Arnold, and Lovell, Brian C. Face recognition on consumer devices: Reflections on replay attacks. *IEEE Transactions on Information Forensics and Security*, 10(4): 736–745, 2015.
- Szegedy, Christian, Zaremba, Wojciech, Sutskever, Ilya, Bruna, Joan, Erhan, Dumitru, Goodfellow, Ian J., and Fergus, Rob. Intriguing properties of neural networks. *ICLR*, abs/1312.6199, 2014. URL <http://arxiv.org/abs/1312.6199>.
- Szegedy, Christian, Vanhoucke, Vincent, Ioffe, Sergey, Shlens, Jonathon, and Wojna, Zbigniew. Rethinking the inception architecture for computer vision. *CoRR*, abs/1512.00567, 2015. URL <http://arxiv.org/abs/1512.00567>.